Impact of Strong ENSO on Regional Tropical Cyclone Activity in a High-Resolution Climate Model in the North Pacific and North Atlantic Oceans

Lakshmi Krishnamurthy

National Oceanic and Atmospheric Administration/Geophysical Fluid Dynamics Laboratory, Princeton, New Jersey, and University Corporation for Atmospheric Research, Boulder, Colorado

Gabriel A. Vecchi

National Oceanic and Atmospheric Administration/Geophysical Fluid Dynamics Laboratory, and Atmospheric and Oceanic Sciences Program, Princeton University, Princeton, New Jersey

Rym Msadek

National Oceanic and Atmospheric Administration/Geophysical Fluid Dynamics Laboratory, Princeton, New Jersey, and University Corporation for Atmospheric Research, Boulder, Colorado

Hiroyuki Murakami

National Oceanic and Atmospheric Administration/Geophysical Fluid Dynamics Laboratory, and Atmospheric and Oceanic Sciences Program, Princeton University, Princeton, New Jersey

Andrew Wittenberg and Fanrong Zeng

National Oceanic and Atmospheric Administration/Geophysical Fluid Dynamics Laboratory, Princeton, New Jersey

(Manuscript received 7 July 2015, in final form 19 December 2015)

ABSTRACT

Tropical cyclone (TC) activity in the North Pacific and North Atlantic Oceans is known to be affected by the El Niño–Southern Oscillation (ENSO). This study uses the GFDL Forecast Oriented Low Ocean Resolution Model (FLOR), which has relatively high resolution in the atmosphere, as a tool to investigate the sensitivity of TC activity to the strength of ENSO events. This study shows that TCs exhibit a nonlinear response to the strength of ENSO in the tropical eastern North Pacific (ENP) but a quasi-linear response in the tropical western North Pacific (WNP) and tropical North Atlantic. Specifically, a stronger El Niño results in disproportionate inhibition of TCs in the ENP and North Atlantic, and leads to an eastward shift in the location of TCs in the southeast of the WNP. However, the character of the response of TCs in the Pacific is insensitive to the amplitude of La Niña events. The eastward shift of TCs in the southeast of the WNP in response to a strong El Niño is due to an eastward shift of the convection and of the associated environmental conditions favorable for TCs. The inhibition of TC activity in the ENP and Atlantic during El Niño is attributed to the increase in the number of days with strong vertical wind shear during stronger El Niño events. These results are further substantiated with coupled model experiments. Understanding of the impact of strong ENSO on TC activity is important for present and future climate as the frequency of occurrence of extreme ENSO events is projected to increase in the future.

Corresponding author address: Lakshmi Krishnamurthy, NOAA/Geophysical Fluid Dynamics Laboratory, Princeton University Forrestal Campus, 201 Forrestal Rd., Princeton, NJ 08540-6649.
E-mail: Lakshmi.Krishnamurthy@noaa.gov

1. Introduction

Tropical cyclones (TCs) are one of the deadliest natural disasters causing intense damage to human life and property (Landsea 2000; Peduzzi et al. 2012; Pielke et al. 2008). Thus, there is interest in predicting

TCs, particularly to help support decisions. Scientists have been researching for predictors of TCs for several decades. The El Niño–Southern Oscillation (ENSO) phenomenon has been shown to exhibit considerable influence on TCs through changes in the thermodynamic factors and large-scale circulation (Gray 1984; Goldenberg and Shapiro 1996; Chia and Ropelewski 2002; Wang and Chan 2002; Tang and Neelin 2004; Vimont and Kossin 2007; Kim et al. 2011; Kim et al. 2014; Vecchi et al. 2014; H. Wang et al. 2014; Murakami et al. 2015; Villarini et al. 2014). Pielke and Landsea (1999) indicate that the state of the tropical Pacific has a significant influence on the probability of losses exceeding $1 billion (U.S. dollars) in the United States caused by TCs. The probability of landfall of TCs over the United States is significantly higher during La Niña than El Niño (Bove et al. 1998) and the spatial distribution of TC-related flooding was shown to depend on the phase of ENSO (Villarini et al. 2014).

Climate change studies suggest that ENSO may undergo significant changes in the next century with an increase in extreme El Niño and La Niña events in response to increased greenhouse gas concentrations (Power et al. 2013; Cai et al. 2014, 2015; Wittenberg 2015). Thus, it is important to examine the response of regional TCs to changes in the state of the tropical Pacific Ocean either caused by climate change or other factors. Further, evaluation of the ability of current generation coupled climate models in simulating these changes in the ENSO–TC relation in different ocean basins in response to the changes in the strength of ENSO could advance our ability to predict the variations in TCs using these models.

Several studies have analyzed the effect of ENSO on TC activity in the Pacific and Atlantic Oceans. ENSO affects the genesis, tracks, intensity, and lifetime of TCs in the West North Pacific (WNP), the central to east North Pacific (ENP), and the North Atlantic, through the regional changes in sea surface temperature (SST), vertical wind shear (VWS), extension of the monsoon trough, and relative vorticity induced by the wind anomalies in the lower troposphere and changes in the upper-tropospheric temperatures (Wang and Chan 2002; Chia and Ropelewski 2002; Gray 1984; Shapiro 1987; Goldenberg and Shapiro 1996; Tang and Neelin 2004). El Niño favors the genesis of TCs in the southeast of the WNP and inhibits in the northwest of the WNP (Chan 1985; Dong 1988; Chia and Ropelewski 2002). Thus, TCs have higher probability to hit Japan, Korea, and northern China during La Niña years compared to El Niño years (Kim et al. 2011). In contrast, the likelihood of TCs reaching

Hawaii is higher during El Niño events than during La Niña (Schroeder and Yu 1995; Irwin and Davis 1999; Wu and Lau 1992; Chu 2004). This is due to El Niño causing a westward shift of the genesis location of TCs in the ENP, which enhances the formation of TCs in the central Pacific (Schroeder and Yu 1995; Irwin and Davis 1999; Wu and Lau 1992) in addition to extending their lifetime (Chu 2004). The influence of El Niño occurs through the increase in the cyclonic vorticity, the decrease in VWS, and the enhancement of the moist layer depth due to the boundary layer convergence (Chu 2004).

In the North Atlantic, El Niño inhibits the formation of TCs through the enhancement of the VWS, subsidence, and reduced relative humidity in the tropical Atlantic (Gray 1984; Shapiro 1987; Goldenberg and Shapiro 1996; Camargo et al. 2007; Chu 2004). El Niño also induces warm tropospheric temperatures over the North Atlantic causing disequilibrium with the North Atlantic SSTs and thus creating an unfavorable environment for the formation of TCs (Tang and Neelin 2004). In addition, observational and model studies have explored the effect of different flavors of ENSO on TC activity such as the east Pacific warming (canonical El Niño) and central Pacific warming (El Niño Modoki) (Kim et al. 2009; Chen 2011; Zhang et al. 2012; Wang et al. 2013; X. Wang et al. 2014; Li and Wang 2014). El Niño Modoki favors the formation of TCs over the South China Sea and southeast of Japan in contrast to the canonical El Niño that creates unfavorable conditions (Chen and Tam 2010; Chen 2011). In the North Atlantic, El Niño Modoki increases the frequency and landfall potential of TCs along Central America and the coast of the Gulf of Mexico (Kim et al. 2009; H. Wang et al. 2014).

These earlier studies have focused only on the effect of different phases of ENSO (El Niño and La Niña) and on the effect of their relative shift in the location of SST anomalies (canonical ENSO or Modoki ENSO) on TCs. The effect of changes in the strength of ENSO on TC activity has not been fully explored. Wang and Chan (2002) have attempted to understand the effect of ENSO strength on regional TC activity in the WNP. Considering that the extreme ENSO precipitation events are suggested to increase in the coming century in response to an increased ENSO amplitude (Power et al. 2013; Wittenberg 2015; Cai et al. 2014, 2015) and given that the amplitude of ENSO exhibits multidecadal variability (e.g., Wittenberg 2009), it is important to understand the changes in the ENSO teleconnections such as the regional TC activity in the Pacific and Atlantic Oceans associated with stronger ENSO events. To overcome the challenge of limited sample size in observations, we make use of long control simulations from

Geophysical Fluid Dynamics Laboratory (GFDL) Forecast Oriented Low Ocean Resolution Model (FLOR) to investigate the sensitivity of TCs to the strength of ENSO. The observations that are used, the details of the model and model experiment, and the methodology used are described in section 2. Results from this investigation are presented in section 3. The conclusions and discussion are presented in section 4.

2. Data and method of analysis

a. Observations

We use SST data from HadISST1.1 from the Hadley Centre for Climate Prediction and Research. The SST data span over the period 1870–2013 and are available on $1° \times 1°$ grid (Rayner et al. 2003). The zonal winds are from NASA's Modern-Era Retrospective Analysis for Research and Applications (MERRA) high-resolution reanalysis data. They comprise zonal winds on $0.5° \times 0.5°$ in longitude × latitude for the period 1979–2013 at 42 vertical levels (Rienecker et al. 2011). The precipitation data are obtained from the Climate Prediction Center (CPC) Merged Precipitation analysis (CMAP) at http://www.esrl.noaa.gov/psd/ (Xie and Arkin 1997). They are available on $2.5° \times 2.5°$ grid and for the period 1979–2013. The TC data are obtained from the International Best Track Archive for Climate Stewardship (IBTrACS). From the IBTrACS collection (Knapp et al. 2010), we choose data from the Joint Typhoon Warning Center for the west Pacific Ocean and from the National Hurricane center for the east Pacific and Atlantic Oceans for the period 1979–2012.

b. Model and experiment

We make use of a coupled climate model developed at GFDL, FLOR, which has high-resolution atmosphere and land components at $0.5° \times 0.5°$ spatial resolution and 32 vertical levels. The oceanic component is at $1°$ resolution. Details on the FLOR model can be found in Vecchi et al. (2014) and Jia et al. (2015). We use 600 years of data from the FLOR 1990 control simulation. It has been shown in Vecchi et al. (2014) that the FLOR model has biases in simulating the observed ENSO–TC relationship in the Pacific and Atlantic Oceans. Thus, we also analyze 500 years of data from a flux-adjusted version of FLOR (FLOR-FA). The FLOR-FA run is also described in Vecchi et al. (2014). In FLOR-FA, the SST and wind stress are adjusted toward observed estimates to improve the mean climate state, which in turn translates into better simulation of climate variability, teleconnections, and

forecasts of some major climate features compared to FLOR (Vecchi et al. 2014; Krishnamurthy et al. 2015; A. T. Wittenberg et al. 2014, unpublished manuscript; Delworth et al. 2015). We perform a restoring SST experiment, to explore the hypothesis that the differences in the ENSO–TC teleconnection between FLOR and FLOR-FA arise from differences in the strength of ENSO. In this experiment, the tropical Pacific SSTs in FLOR are restored to FLOR monthly climatology repeating every year plus the monthly anomalies from FLOR-FA (hereafter referred as FLOR_FA-enso). The rest of the oceans are fully coupled wherein the atmosphere responds to the ocean-generated SSTs. This experiment is run for 100 years. Further details on this experiment can be found in Krishnamurthy et al. (2015).

c. Method of analysis

To focus on regional TC activity, our main index of TC activity is TC track density (for brevity we use TC density to refer to TC track density throughout the manuscript). The TC track density is calculated as follows. Tropical cyclones are detected based on the algorithm used in Zhao et al. (2009) with modifications in the detection criteria. In the first step, a potential storm at a location is identified using 6-hourly data, which satisfies the criteria that the relative vorticity at 850 hPa exceeds $3.5 \times 10^{-5}\,s^{-1}$ within $6° \times 6°$ domain, and is associated with a local minimum in sea level pressure and a warm core center within a distance of $2°$ latitude × $2°$ longitude limit. Using this potential storm data, the storm trajectory is determined where the trajectory lasts at least 3 days and has a maximum wind speed greater than $15.3\,m\,s^{-1}$. We choose the $15.3\,m\,s^{-1}$ threshold based on the 90% scale on the observed threshold for the 50-km model resolution based on Walsh et al. (2007). Based on this, the threshold for gale-force winds is $15.3\,m\,s^{-1}$ in FLOR (Vecchi et al. 2014). Further, TC density and genesis density are calculated from this data based on the methodology defined in Vecchi et al. (2014). The density is determined on $1° \times 1°$ resolution. The number of TCs passing through the $10° \times 10°$ box surrounding each $1° \times 1°$ grid point at every 6-h interval is counted and divided by 4 to obtain the storm days. The data are finally smoothed to obtain TC density.

We have also employed composite analysis in this study and the composites are tested for their significance using a resampling bootstrap method (Chu and Wang 1997; Chen 2011). We performed a significance test to determine if the TC density during El Niño years is significantly different from non–El Niño years. For the procedure of significance test we follow the resampling
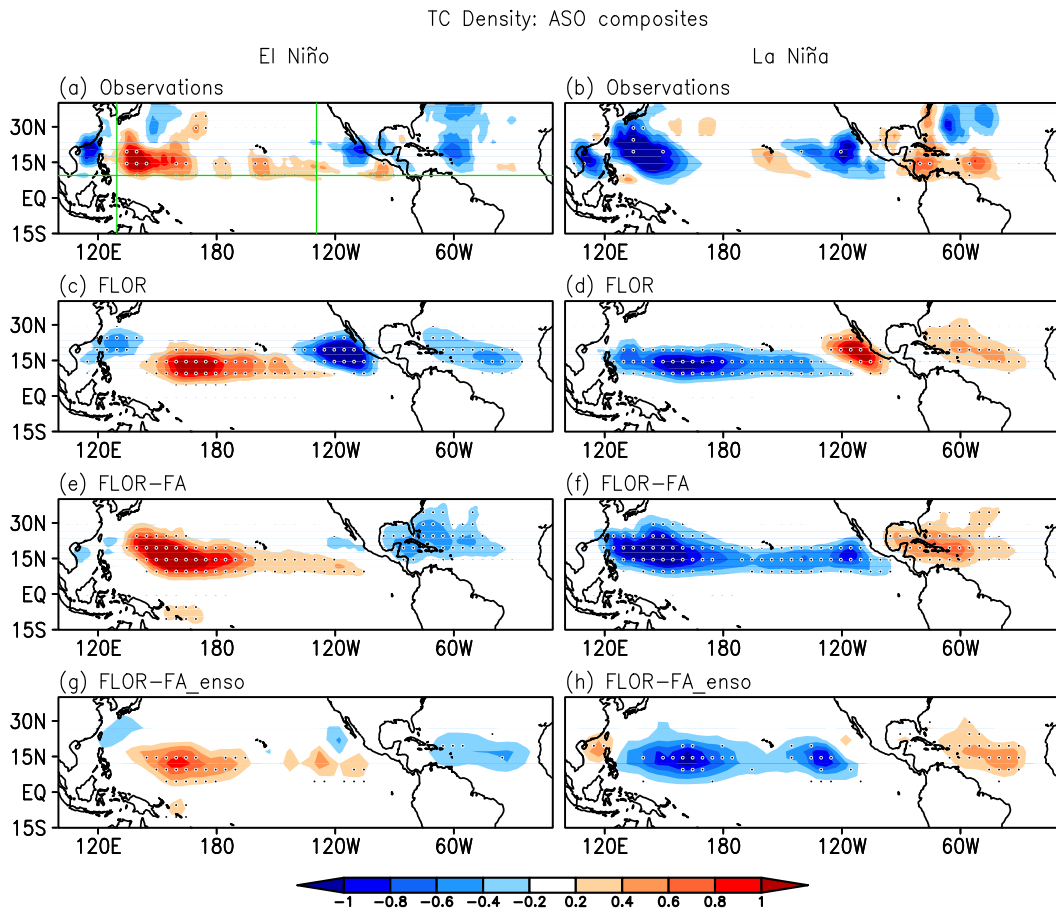
FIG. 1. ASO seasonal composites of TC density for (a) observations, (c) FLOR, (e) FLOR-FA, and (g) FLOR-FA_ enso for El Niño. (b),(d),(f), (h) As in (a),(c),(e),(g), but for La Niña. The criteria for El Niño (La Niña) composites is based on ASO seasonal Niño-3.4 greater (less) than 1.0 SD (−1.0 SD). The number of years over which composites are based is noted in Table 1. The dotted regions indicate 5% significance level. The regions marked by green lines north of 10°N correspond to the North Pacific and North Atlantic TC activity. In regions west of 130°E, east of 130°E, and east of 130°W in the Pacific are referred to as northwest of WNP, southeast of WNP, and ENP, respectively. The unit for TC density is the number of tropical cyclones per season in a 1° × 1° grid box.

and permutation method suggested in Chu and Wang (1997) and Chen (2011).

This test involves the following null hypothesis and alternative hypothesis,

$$H_0: \mu_i = \mu_j \quad H_1: \mu_i \neq \mu_j, \qquad (1)$$

where, μ_i is the mean of the El Niño sample and μ_j is the mean of the non–El Niño sample.

Following the technique in Chu and Wang (1997) and Chen (2011), we resample the data to group into new set of El Niño and non–El Niño years. The test statistic as below is computed:

TABLE 1. Number of years associated with Niño-3.4 greater than 1.0 SD (second column) and with less than −1.0 SD (fourth column). Rate of occurrence of El Niño and La Niña events per year with a binomial estimate of uncertainty is shown for El Niño (third column) and La Niña (fifth column), respectively. The years corresponding to El Niño are 1982, 1987, 1997, 2002, 2004, and 2009, and those corresponding to La Niña are 1988, 1998, 1999, and 2007 in observations.

Data	El Niño	Rate of El Niño	La Niña	Rate of La Niña
Observations	6	0.17 ± 0.12	4	0.11 ± 0.10
FLOR	108	0.18 ± 0.03	110	0.18 ± 0.03
FLOR-FA	47	0.09 ± 0.02	54	0.10 ± 0.02
FLOR-FA_enso	15	0.15 ± 0.06	18	0.18 ± 0.07

$$U = \frac{\sqrt{n_i + n_j - 2}(x_i - x_j)}{\sqrt{(n_i - 1)\,\text{var}_i + (n_j - 1)\,\text{var}_j/\text{kk}}\sqrt{\left(\dfrac{1}{n_i} + \dfrac{\text{kk}}{n_j}\right)}}, \quad (2)$$

where n is the sample size, x is mean, var is variance, kk is sample variance, i refers to the El Niño sample, and j refers to the non–El Niño sample in Eqs. (1) and (2). This test statistic in Eq. (2) is based on the assumption that the variances of two batches are not equal but their ratio is known.

We repeat the above procedure 1000 times and create a distribution of U statistic of resampled data. If the U statistic value of actual data lies outside of the 95% level of the distribution, we reject the null hypothesis at the 5% level.

3. Results

a. ENSO-related TC activity

We first assess the ability of FLOR to capture the observed ENSO–TC relationship. We show the composites of TC density for both the warm and cold phases of ENSO during August–September–October (ASO) based on the standardized Niño-3.4 index (Fig. 1). We choose the ASO season, as this is the common peak season over which TCs occur over the west North Pacific, central to the east North Pacific and the North Atlantic basins. Years with standardized Niño-3.4 exceeding +1.0 standard deviation (SD) are considered as El Niño years and those with Niño-3.4 below −1.0 SD are considered as La Niña years. The number of years included in each composite for observations and model are given in Table 1. The comparison of the composites between El Niño and La Niña highlights the nonlinearity in the ENSO–TC relation. During El Niño, the observed composite (Fig. 1a) suggests reduced TC activity off the coast in the WNP, ENP, and tropical North Atlantic, and increased TC activity west of the date line in the WNP and central Pacific. La Niña has the opposite effect on TC activity to the west of the date line in the WNP and the tropical Atlantic (Fig. 1b), suggesting linearity in the teleconnection in these regions. However, La Niña leads to a reduction in TC activity in the far WNP (over the South China Sea) and ENP similar to El Niño, suggesting nonlinearity in these regions.

The ENSO-related TC activity in FLOR is different from observations with an erroneous eastward extension of enhanced TC activity during El Niño and reduced activity in the southeast of the WNP extending into the central Pacific during La Niña that is not observed (Figs. 1c and 1d). The magnitude of suppression of TC activity in the west Atlantic during El Niño years and the
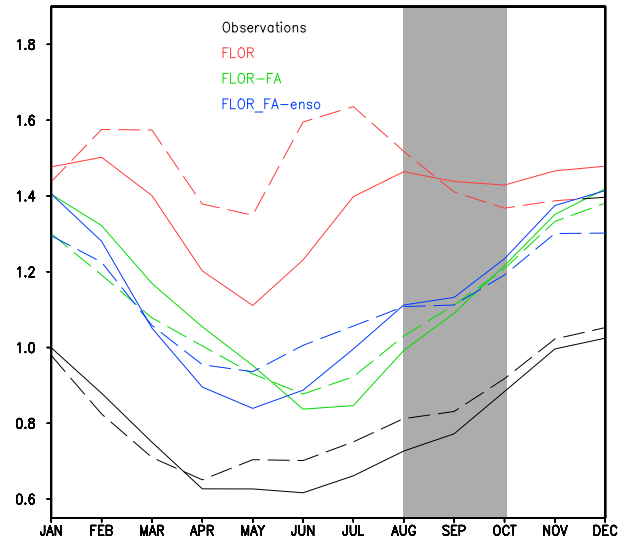

FIG. 2. Standard deviation of monthly Niño-3.4 for observations (solid black), FLOR, (solid red), FLOR-FA (solid green), and FLOR_FA-enso (solid blue). The dashed curves, are as in Niño-3.4, but for Niño-3.

enhancement during La Niña years is weaker in FLOR relative to observations (Figs. 1c and 1d). In the ENP, El Niño in FLOR leads to an excessive inhibition of TC activity and La Niña is associated with an increase in activity, in contrast to a reduced activity in observations. Meanwhile, consistent with Vecchi et al. (2014), FLOR-FA shows an improvement relative to FLOR in the simulation of both the El Niño– and La Niña–related TC activity in the Pacific and Atlantic Oceans. The marked improvements in the southeast of WNP and the ENP are present during both El Niño and La Niña events.

Comparison of SSTs in the tropical Pacific and regional TC density suggests that the differences in the simulation of the ENSO–TC relationship in FLOR relative to observations and FLOR-FA may arise from a too strong ENSO in FLOR (Vecchi et al. 2014; Krishnamurthy et al. 2015). The monthly standard deviation of Niño-3.4[1] indicates that the magnitude of ENSO is higher in FLOR than in observations and FLOR-FA (Fig. 2). The strength of ENSO is improved in FLOR-FA, and it was hypothesized in Vecchi et al. (2014) that this may lead to improvements in the ENSO–TC teleconnection. The model simulates realistic TC response to ENSO, although the strength of ENSO is slightly higher than observations. Restoring the FLOR SST anomalies in the tropical Pacific to the

---

[1] We have also compared the strength of ENSO among observations, FLOR, and FLOR-FA using the Niño-3 index and show similar results.
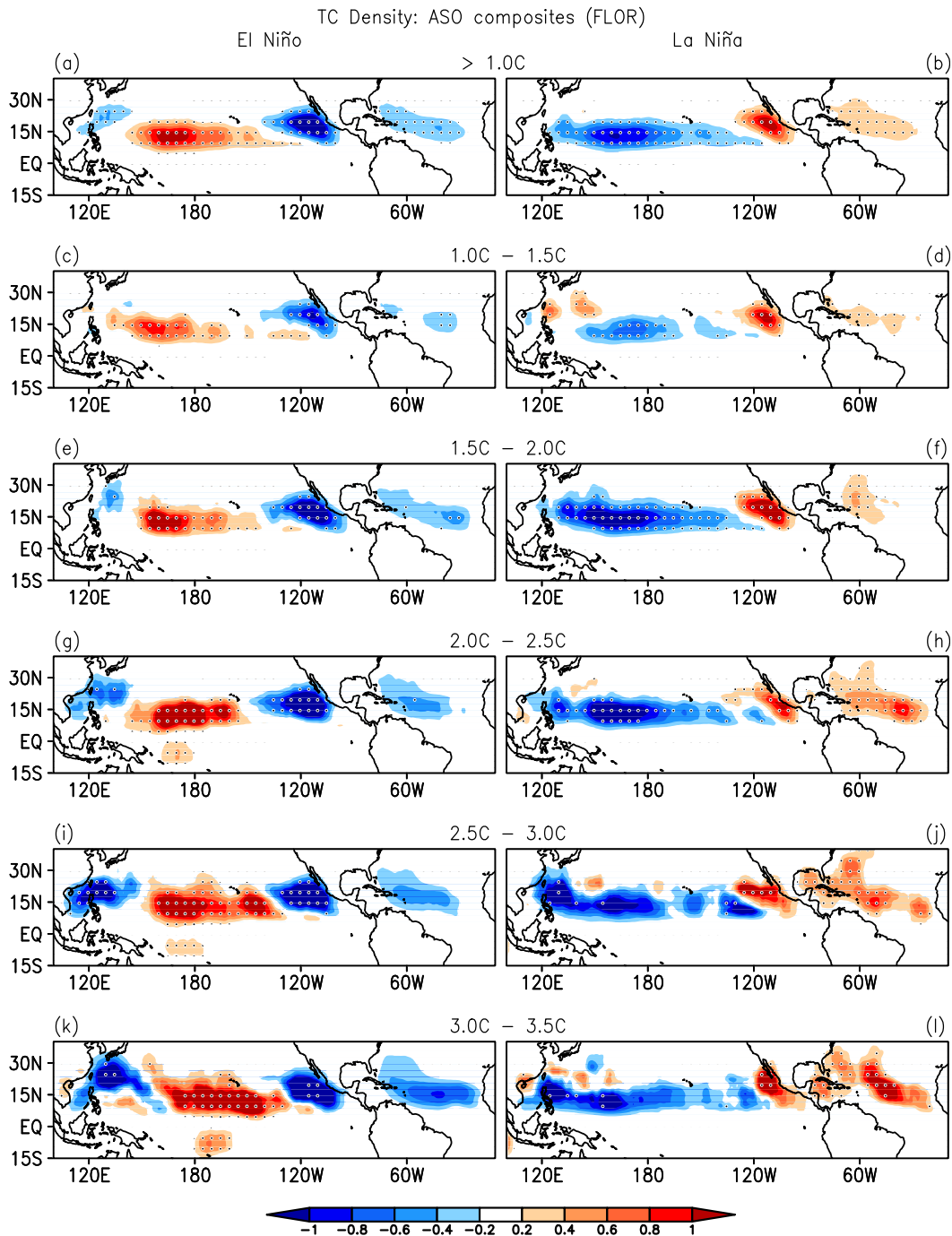
FIG. 3. ASO composites of TC density for FLOR based on Niño-3.4 (a) greater than 1°C, (c) between 1.0° to 1.5°C, (e) between 1.5° to 2.0°C, (g) between 2.0° to 2.5°C, (i) between 2.5° to 3.0°C, and (k) between 3.0° to 3.5°C for El Niño. La Niña composites are based on Niño-3.4 (b) less than −1.0°C, (d) between −1.0° and −1.5°C, (f) between −1.5° and −2.0°C, (h) between −2.0° and −2.5°C, (j) between −2.5° and −3.0°C, and (l) between −3.0° and −3.5°C. The number of years over which composites are based is noted in Table 2. The dotted regions indicate the 5% significance level. The unit for TC density is the number of tropical cyclones per season in a 1° × 1° grid box.

TABLE 2. Number of years (second column) associated with each composite criterion of Niño-3.4 (first column) for FLOR for El Niño composite. For the La Niña composite, the criteria are negative values of the temperatures in the first column and the corresponding number of years is listed in fourth column. Rate of occurrence of El Niño and La Niña events per year with a binomial estimate of uncertainty is shown for El Niño (third column) and La Niña (fifth column), respectively.

Criteria	El Niño	Rate of El Niño	La Niña	Rate of La Niña
>1.0°C	136	0.22 ± 0.03	141	0.23 ± 0.03
1.0°–1.5°C	52	0.08 ± 0.02	53	0.08 ± 0.02
1.5°–2.0°C	35	0.05 ± 0.01	47	0.05 ± 0.01
2.0°–2.5°C	23	0.03 ± 0.01	27	0.04 ± 0.01
2.5°–3.0°C	20	0.03 ± 0.01	7	0.01 ± 0.008
3.0°–3.5°C	6	0.01 ± 0.007	6	0.01 ± 0.007

TABLE 3. As in Table 2, but for FLOR-FA.

Criteria	El Niño	Rate of El Niño	La Niña	Rate of La Niña
>1.0°C	78	0.15 ± 0.03	77	0.15 ± 0.03
1.0°–1.5°C	42	0.08 ± 0.02	38	0.07 ± 0.02
1.5°–2.0°C	25	0.05 ± 0.01	25	0.05 ± 0.01
2.0°–2.5°C	7	0.014 ± 0.01	10	0.02 ± 0.01
2.5°–3.0°C	3	0.006 ± 0.006	3	0.006 ± 0.006

SST anomalies from FLOR-FA (which by construction produces a similar amplitude of ENSO as that of FLOR-FA) supports this hypothesis (Figs. 1g,h). The marginal improvement in the WNP may highlight the importance of the mean state in addition to the magnitude of SST anomalies. In this study we focus on the sensitivity of TCs to the magnitude of SST anomalies.

In the next sections, we explore this hypothesis that strong ENSO events contribute to differences in response of the TC activity to ENSO in FLOR, FLOR-FA, and observations. We also analyze the underlying mechanisms for the sensitivity of TCs to incremental changes in the strength of ENSO. Since FLOR-FA successfully simulates the observed TCs and its teleconnection with ENSO, in the following, we use FLOR-FA as a reference (instead of observations) to evaluate FLOR.

b. Sensitivity of TCs to the strength of ENSO

To explore the sensitivity of TC activity to the magnitude of ENSO events, we analyze composites of TC density based on the magnitude of Niño-3.4[2] SST anomalies. The composites of TC density for El Niño years are constructed over years for which Niño-3.4 is between 1.0°–1.5°C, 1.5°–2.0°C, 2.0°–2.5°C, 2.5°–3.0°C, and 3.0°–3.5°C. The composite computed for all years during which Niño-3.4 is greater than 1°C is also shown (Fig. 3a) to compare with the composite based on years with standardized Niño-3.4 greater than one standard

deviation (Fig. 1c) and the comparison suggests that they have a close resemblance. Similarly, we define composites for La Niña years using below-normal Niño-3.4 temperatures. The number of years included in each composite for FLOR and FLOR-FA are tabulated in Tables 2 and 3, respectively. Since FLOR-FA shows improvement in the simulation of ENSO amplitude and does not show as excessive ENSO amplitude as in FLOR, it does not indicate ENSO events with Niño-3.4 index greater than or less than 3° and −3°C, respectively.

The TC activity related to El Niño shows stronger sensitivity to the strength of ENSO in the southeast of the WNP, ENP, and the Atlantic (cf. Figs. 3c,e,g,i,k). The sensitivity of TCs in the North Atlantic needs to be interpreted with caution, as the values are not significant. The stronger El Niño results in disproportionate inhibition of TC activity off the coast in the WNP and ENP, and an eastward shift in the longitudinal location of TCs from the southeast of WNP to the central Pacific. Strong La Niña events do not show such a marked impact on TC activity in the entire Pacific (cf. Figs. 3d,f,h,j,l), although the WNP tends to show marginal sensitivity in the magnitude up to 2.5°C. This highlights the nonlinearity of the response of TC activity to the strength of ENSO. In the WNP, a strong El Niño leads to a dramatic eastward shift in TCs, which is not necessarily true for strong La Niña events. In the ENP, El Niño leads to a distinct reduction in TCs; however, La Niña does not show such a distinct increase in TCs. The sensitivity of TCs to the strength of La Niña is only seen over the North Atlantic (cf. Figs. 3d,f,h,j,l). FLOR-FA shows a similar sensitivity as FLOR to the strength of ENSO in the southeast of the WNP and the North Atlantic but a more realistic relationship in the ENP compared to observations (cf. Figs. 1a,b,e,f and Fig. 4). The ENP TC activity in FLOR-FA is not as suppressed as in FLOR during El Niño years. Further, during La Niña years, FLOR-FA shows improvements in simulating the suppressed activity in contrast to FLOR where TC activity is enhanced in the ENP. FLOR-FA also has a better simulation of the location of ENSO-related TC activity in the North Atlantic compared to FLOR where TCs are shifted eastward. The reasons for the improved simulation of the ENSO–TC relationship in FLOR-FA and the

---

[2] To have an objective criterion for the strength of ENSO, the composites are constructed based on an absolute value of Niño-3.4 rather than the conventional way of using the standard deviation of Niño-3.4. Assessing the strength of ENSO based on standard deviation would be subjective as the standard deviation of Niño-3.4 varies among observations, FLOR, and FLOR-FA. Using Niño-3 index to define the composites yields similar results.
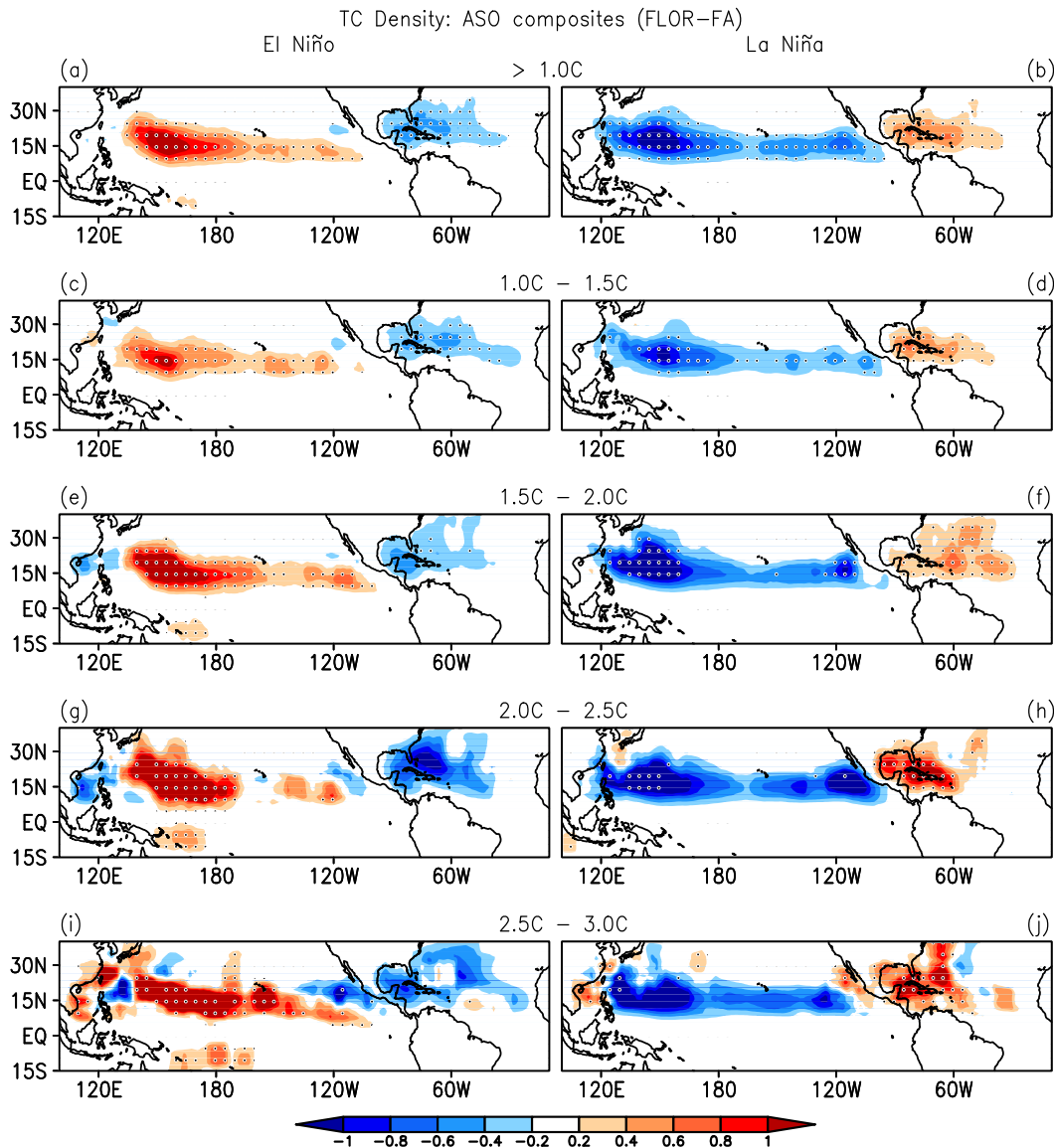
FIG. 4. As in Fig. 3, but for FLOR-FA. The number of years over which composites are based is noted in Table 3. The dotted regions indicate the 5% significance level.

mechanisms for sensitivity of TCs to strong ENSO events are investigated below.

c. Effect of the strength of ENSO on the environmental conditions related to TC activity

To understand the mechanism for the sensitivity of TC activity to the strength of ENSO in different ocean basins, we explore the sensitivity of several environmental factors that are conducive for the formation of TCs, such as, precipitation, sea level pressure, VWS, relative humidity, relative vorticity, and static stability. Among these environmental factors, we find that precipitation and VWS are the main factors that explain the

mechanism for the sensitivity of TC activity to the strength of ENSO in FLOR and FLOR-FA. They also explain the differences in the ENSO–TC relationship between observations, FLOR, and FLOR-FA. Thus, in the following we present only composites related to precipitation and VWS for different strengths of ENSO.

1) WESTERN NORTH PACIFIC

Previous studies have shown that the location of the convection in the tropical Pacific is sensitive to the strength of ENSO. Stronger El Niño is suggested to result in an eastward extension of the convective anomalies (Vecchi and Harrison 2006; Vecchi 2006; Lengaigne and Vecchi
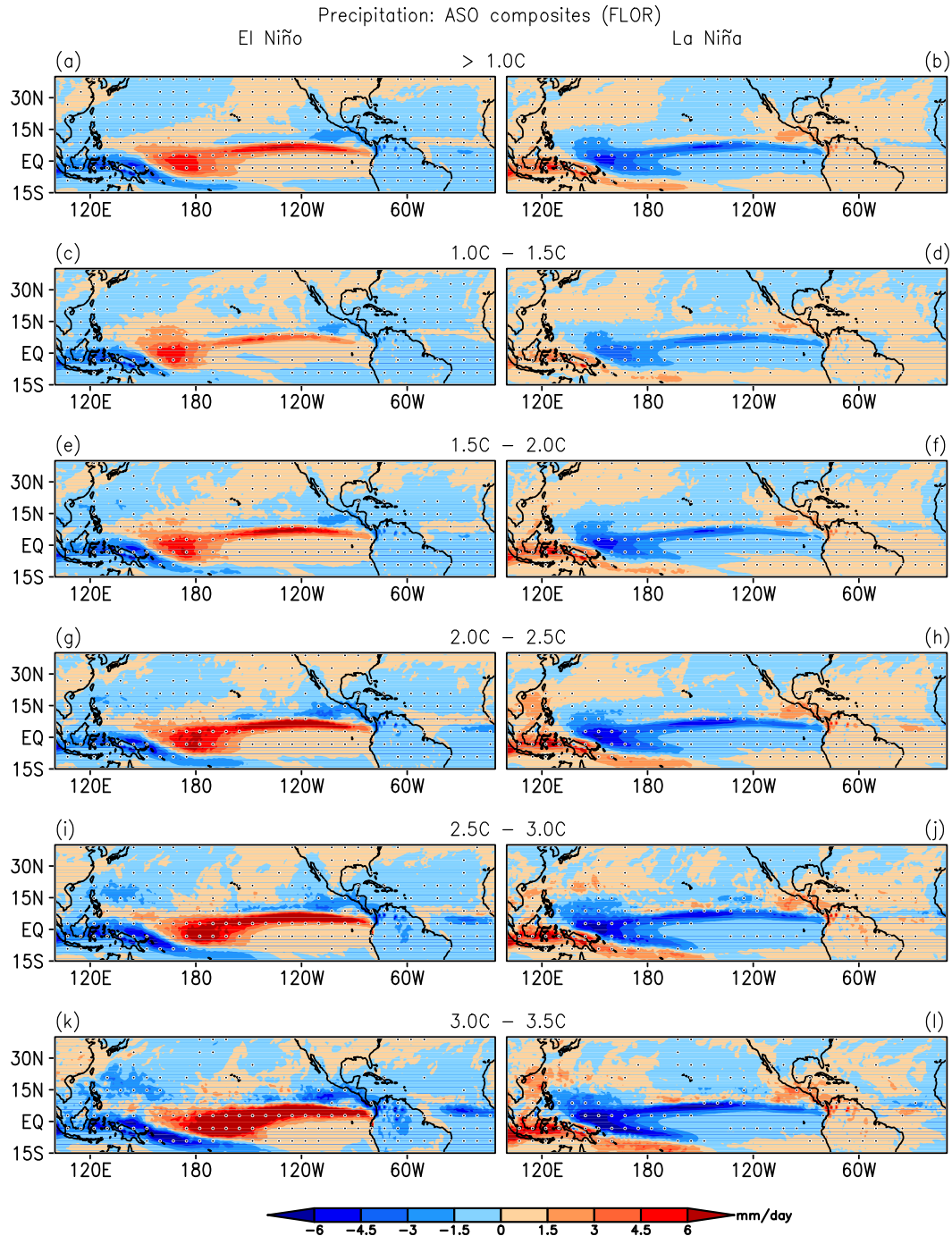
FIG. 5. As in Fig. 3, but that the composites are for precipitation. Units are in mm day^{-1}. The number of years over which composites are based is noted in Table 2. The dotted regions indicate the 5% significance level.

2010). Further, TC response in the WNP is shown to be sensitive to the pattern of precipitation (Murakami et al. 2012). Since TCs are sensitive to the strength and location of precipitation, the shift in convection due to stronger El Niño events may also affect the location of TCs. To explore this hypothesis, we show composites of precipitation

for different strengths of ENSO (Fig. 5). Figure 5 clearly demonstrates that stronger El Niño leads to an eastward shift in convection from the west of the date line to the east of the date line (cf. Figs. 5c,e,g,i,k). The shift in the atmospheric convection is a result of the shift in the Walker circulation associated with an eastward shift in
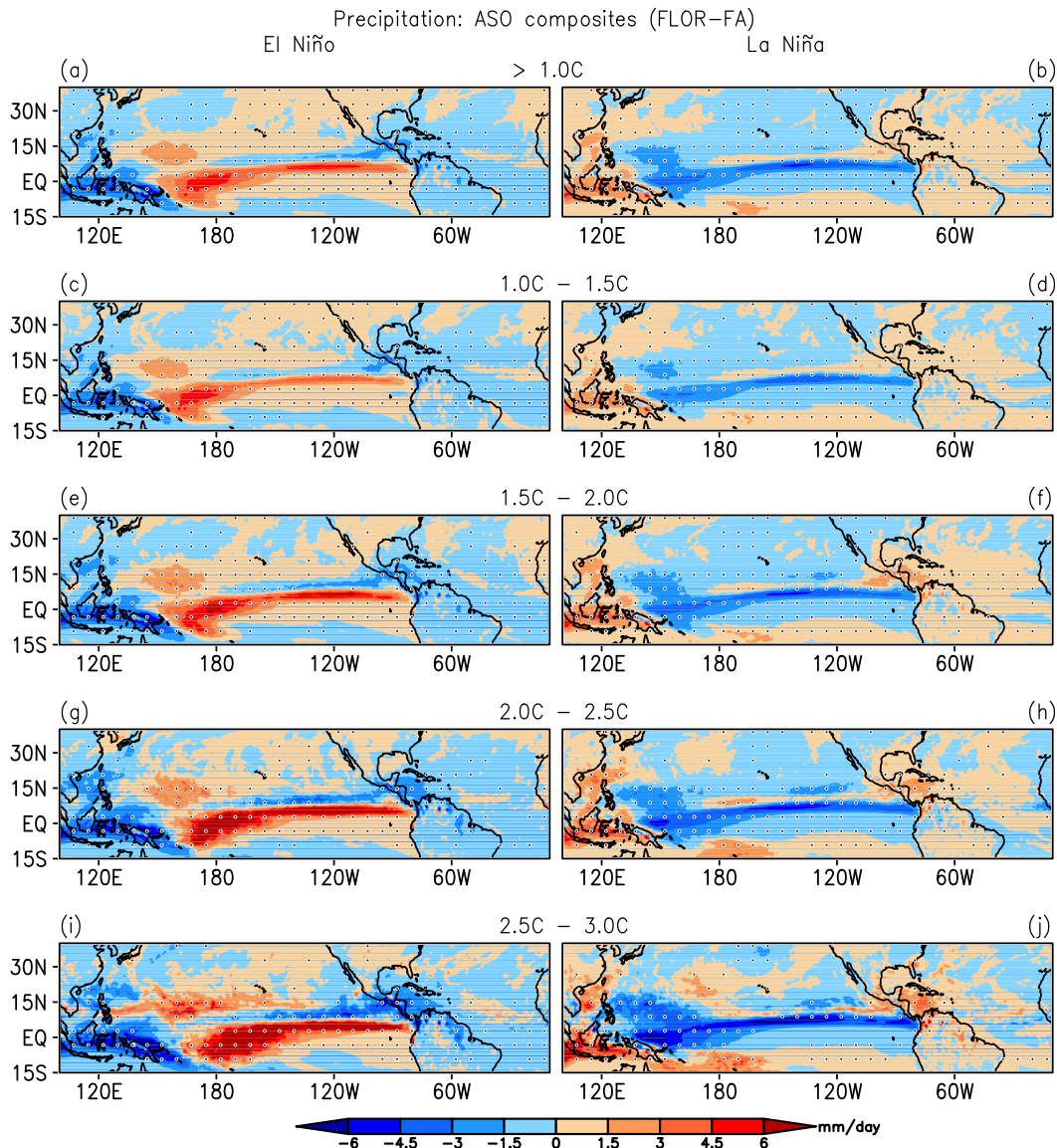
FIG. 6. As in Fig. 5, but for FLOR-FA. The number of years over which composites are based is noted in Table 3. The dotted regions indicate the 5% significance level.

the SST anomalies. The low-level westerlies associated with the Walker circulation also shift eastward and thus lead to a shift in the associated positive relative vorticity and weak VWS anomalies. This eastward shift of the environmental conditions favorable to TCs is consistent with the eastward shift of TCs in the WNP for extreme El Niño cases in FLOR (Fig. 3). This is consistent with Clark and Chu (2002), where low-level vorticity is enhanced and VWS is reduced leading to enhanced TCs during El Niño. We hypothesize that, since FLOR has stronger ENSO variability than observations, the total composite of TCs shows an eastward shift in FLOR relative to observations (cf. Figs. 1a and 1c). FLOR-FA

also suggests such a shift in the convective anomalies for extreme El Niño cases (Fig. 6i) and thus a shift in TC activity in the WNP (Fig. 4i). However, the reduced precipitation anomalies west of the date line associated with La Niña do not show a dramatic eastward shift in the convection with the increase in the strength of ENSO compared to El Niño; hence, the lack of eastward shift in the La Niña–related TC activity (e.g., Figs. 4j and 6j).

2) EASTERN NORTH PACIFIC

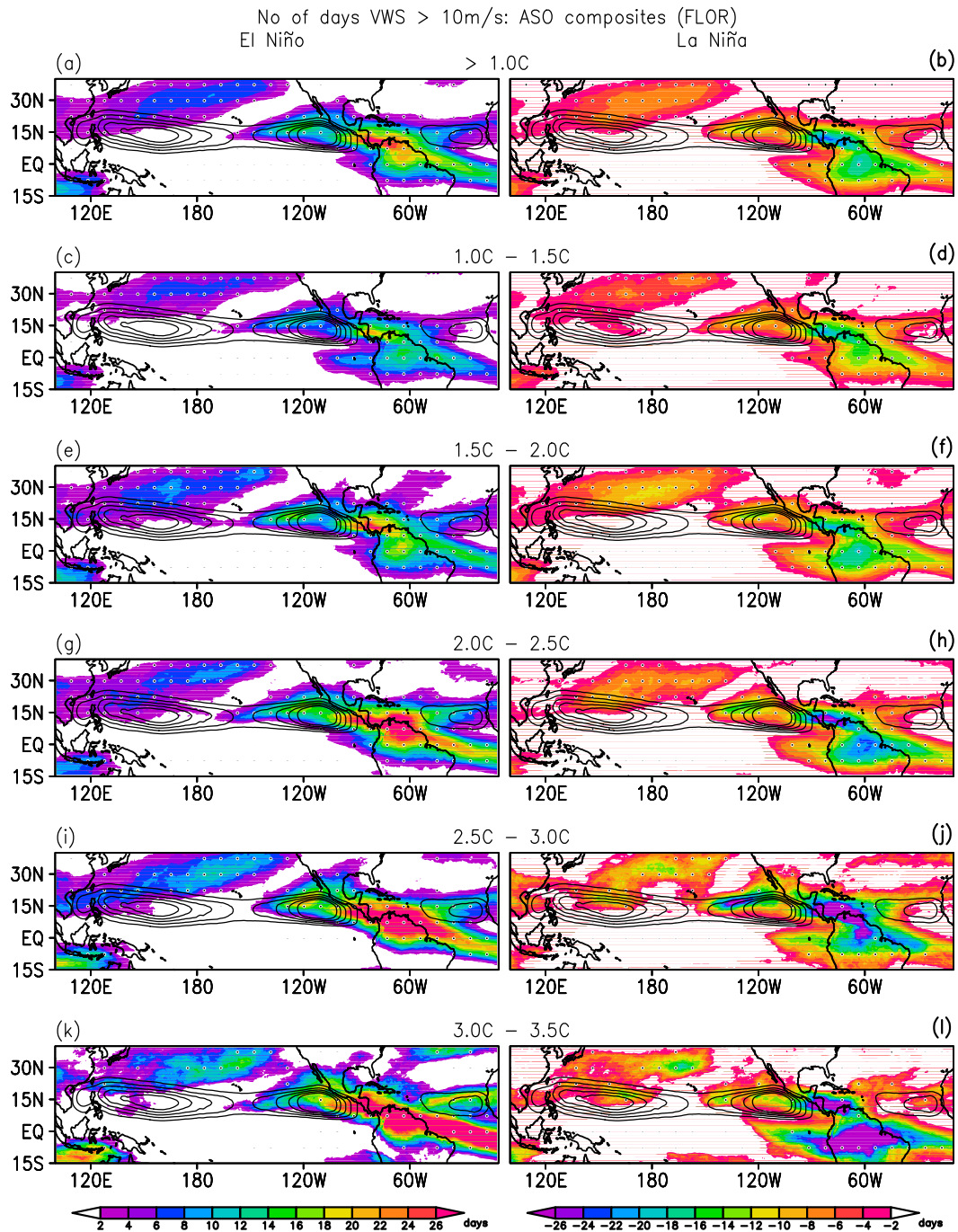As stated in section 3a, FLOR simulates a disproportionate inhibition of TCs relative to observations in

FIG. 7. As in Fig. 3, but that the composites are for number of days the VWS is greater than $10 \, m \, s^{-1}$ in the ASO season. The number of years over which composites are based is noted in Table 2. The dotted regions indicate the 5% significance level. The contours represent climatological genesis density and the contour interval is 0.03.

the ENP during El Niño, while it is realistically simulated in FLOR-FA. We also showed in section 3b that TC activity in the ENP is sensitive to the strength of El Niño and that the suppression is greater for strong El Niño events (e.g., Fig. 3k). Here, we explain the

mechanism for the sensitivity of ENP TCs to the strength of El Niño and the reasons behind the differences in TC activity among FLOR, FLOR-FA, and the observations. Figure 7 shows composites of the number of days with VWS greater than $10 \, m \, s^{-1}$ for different
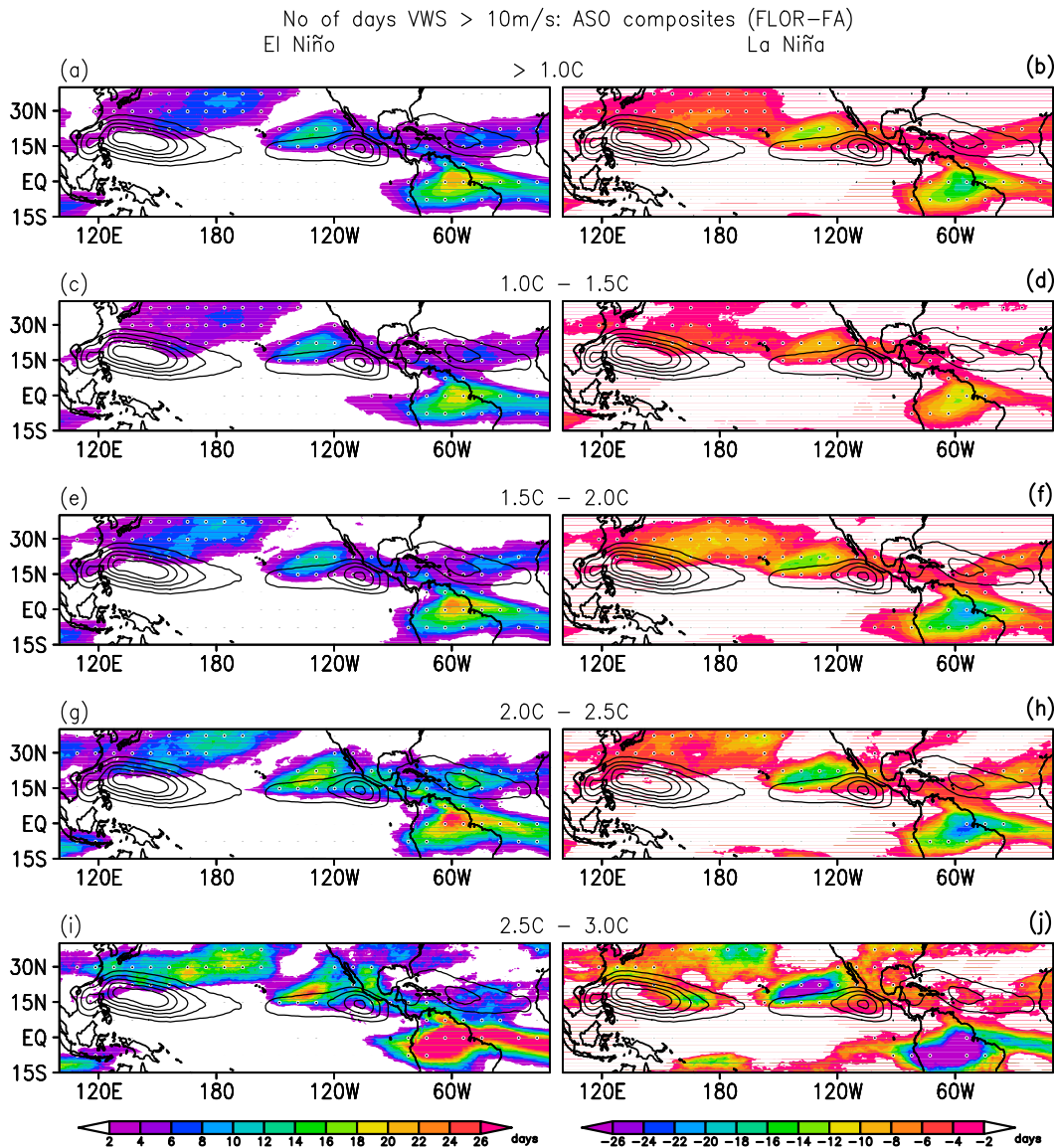
FIG. 8. As in Fig. 7, but for FLOR-FA. The number of years over which composites are based is noted in Table 3. The dotted regions indicate the 5% significance level.

amplitudes of Niño-3.4 with the location of mean genesis density superimposed.[3] For extreme El Niño cases, we notice that the number of days with VWS > $10\,\mathrm{m\,s^{-1}}$ is higher and the regions with a high number of days are collocated with the location of the mean genesis density (cf. Figs. 7c,e,g,i,k). Thus, years with strong El Niño are associated with a larger number of days with

VWS > $10\,\mathrm{m\,s^{-1}}$ during the ASO season creating unfavorable conditions for the formation of TCs. This explains the disproportionate inhibition of TC activity in FLOR in the ENP. In FLOR-FA (Fig. 8), even though stronger El Niño's increase the number of days with VWS > $10\,\mathrm{m\,s^{-1}}$, the location of the high number of days is westward of the mean genesis location; hence, it is unable to suppress TC activity as much as in FLOR.

In sections 3a and 3b, we also showed that La Niña has the opposite effect on the TC activity in the ENP in FLOR in contrast to FLOR-FA and the observations, and that TCs are insensitive to incremental increases in the strength of La Niña. The reasons behind

---

[3] We have verified the composites with the number of days with VWS greater than 4, 6, 8, 10, 12, and $14\,\mathrm{m\,s^{-1}}$. The results are similar with different choices of threshold for strong VWS and thus we show results only for the threshold of $10\,\mathrm{m\,s^{-1}}$.

ASO Climatology

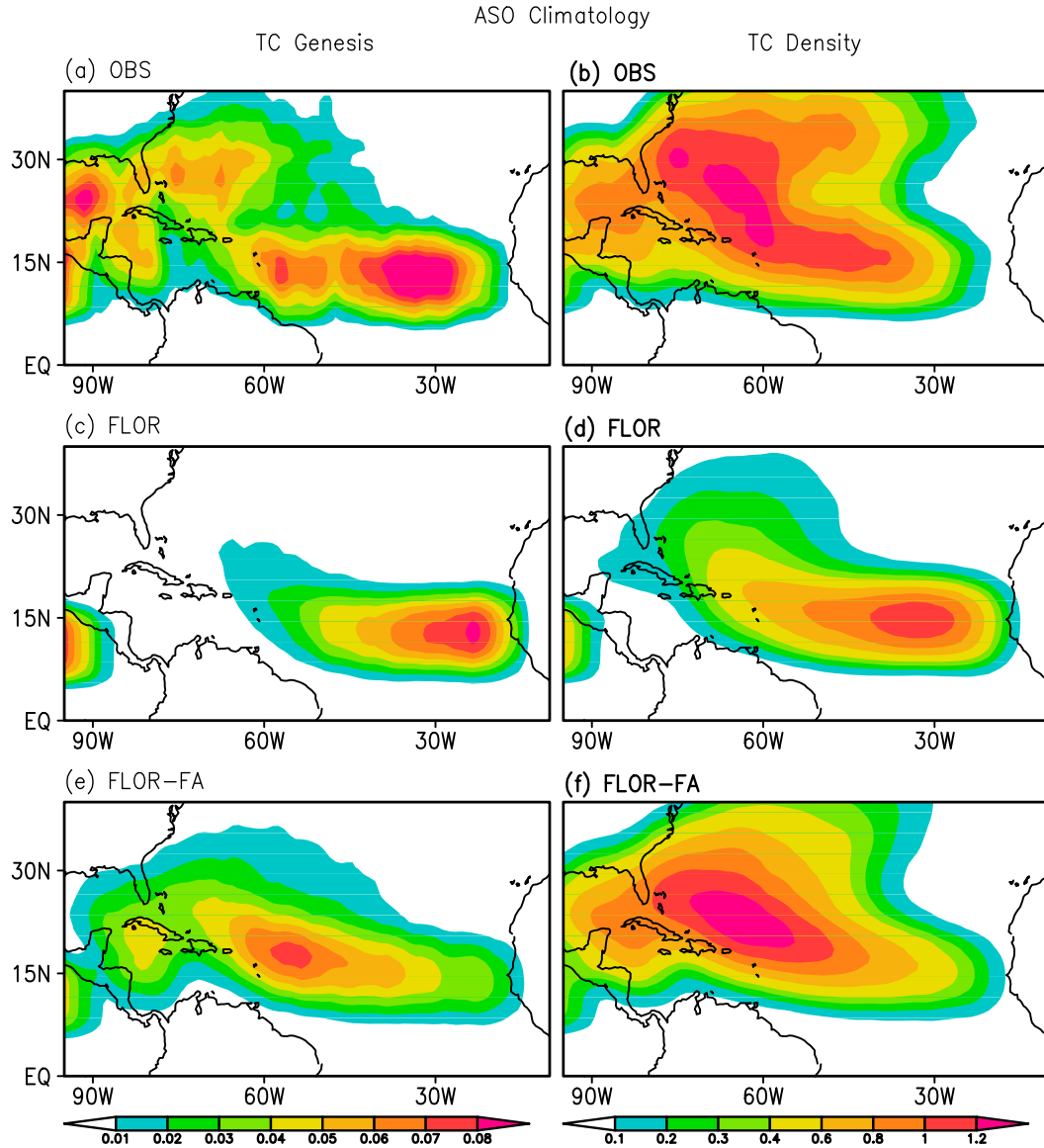TC Genesis   TC Density

FIG. 9. ASO climatology of TC genesis density for (a) observations, (c) FLOR, and (e) FLOR-FA and track density for (b) observations, (d) FLOR, and (f) FLOR-FA.

these effects can also be understood based on the effect of La Niña on VWS. In FLOR, La Niña favors the formation of TCs (Figs. 7b,d,f,h,j,l) by reducing the number of days with VWS $> 10 \, \mathrm{m \, s^{-1}}$ in the mean genesis area. However, in FLOR-FA, the area of reduction is shifted westward of the genesis location; hence, the lack of favorable environmental conditions for the formation of TCs (Figs. 8b,d,f,h,j) similar to observations (cf. Figs. 1f and 4b to Fig. 1b). However, the reasons for inhibition of TCs in FLOR-FA are not understood. The lack of linearity in the mechanism (explained through VWS) for El Niño and La Niña in FLOR-FA may explain the nonlinearity in the effect of

ENSO on the TCs, where both phases lead to a reduction of TCs in the ENP.

3) NORTH ATLANTIC

The TC activity in the North Atlantic has been shown to be sensitive to the strength of both El Niño and La Niña events, with the magnitude of the response increasing with incremental changes in ENSO strength (section 3b). This effect of ENSO on TCs occurs through the changes in VWS in the North Atlantic. In both FLOR and FLOR-FA, the number of days with VWS $> 10 \, \mathrm{m \, s^{-1}}$ increases with the strength of El Niño and is collocated with the mean genesis location creating
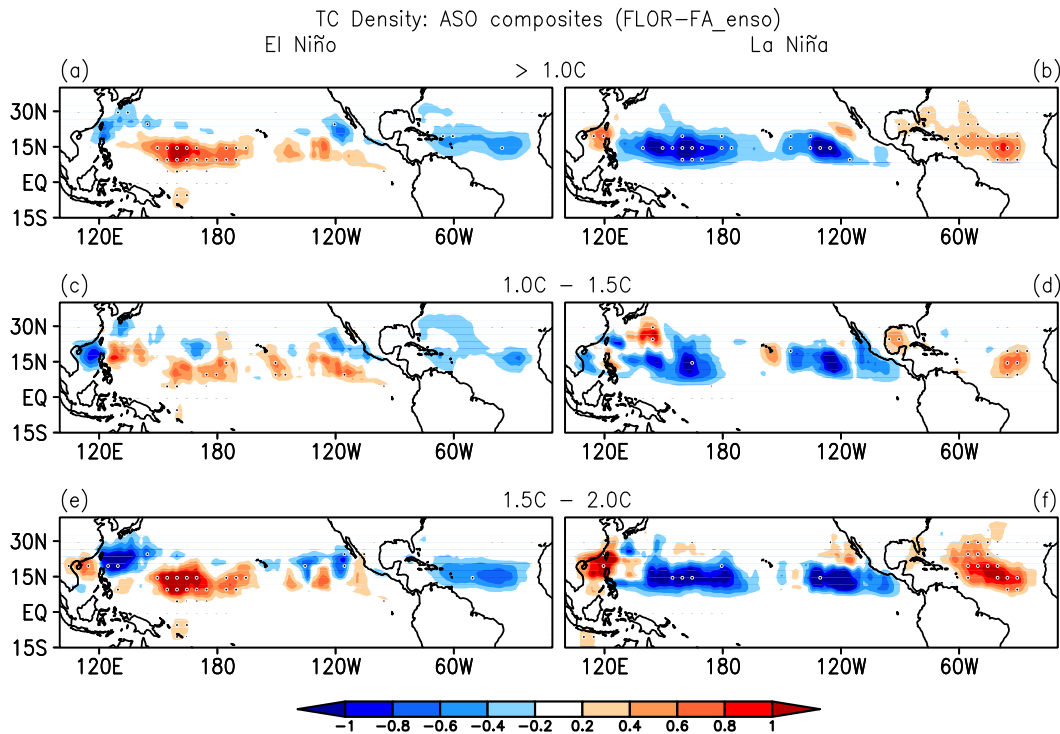
FIG. 10. As in Fig. 3, but for FLOR-FA_enso. The number of years over which composites are based is noted in Table 4. The dotted regions indicate the 5% significance level.

unfavorable conditions for the development of TCs (Figs. 7 and 8). A similar explanation holds for the effect of La Niña except that during La Niña the number of days with VWS > 10 m s^{-1} decreases with the increase in the strength of La Niña and thus it favors TCs (Figs. 7 and 8).

Further, we investigate the reasons for the inability of FLOR to simulate the relationship between ENSO and TC activity in the west Atlantic and the improvement of this relation in FLOR-FA. Examination of the climatological genesis density in FLOR suggests that the model fails to simulate the genesis of TCs in the west Atlantic (Fig. 9c) and thus it has biases in the TC track density (Fig. 9d). However, FLOR-FA shows moderate improvement in the simulation of the genesis (Fig. 9e) and tracks of TCs in the west Atlantic (Fig. 9f). Thus, the lack of relationship between ENSO and TCs in the west Atlantic in FLOR may be attributed to the lack of genesis of TCs in this part of the basin. The lack of genesis in the west Atlantic may be related to the biases in the large-scale climate such as colder SSTs, higher VWS, and lower potential intensity in FLOR compared to observations in the west Atlantic creating unfavorable conditions for TC genesis (Vecchi et al. 2014). These biases are improved in FLOR-FA leading to better simulation of TC genesis.

d. Model experiment

To substantiate that the differences in the simulation of the ENSO–TCs relation in the Pacific arises from differences in the strength of ENSO between FLOR and FLOR-FA, we perform a restoring model experiment (FLOR-FA_enso) using FLOR. This experiment is based on FLOR model and it has SST anomalies in the tropical Pacific in FLOR restored to FLOR-FA anomalies. By construction, the strength of ENSO in FLOR-FA_enso is, therefore, similar to that of FLOR-FA. In this sensitivity experiment, TC activity related to El Niño shows suppressed TCs in the ENP and the northwest of WNP and enhanced TC activity west of the date line (Fig. 10a; Table 4). Although the TC density in the northwest of the WNP does not show dramatic improvement (local mean state may play a role in addition to the magnitude of SST anomalies),

TABLE 4. As in Table 2, but for FLOR-FA_enso.

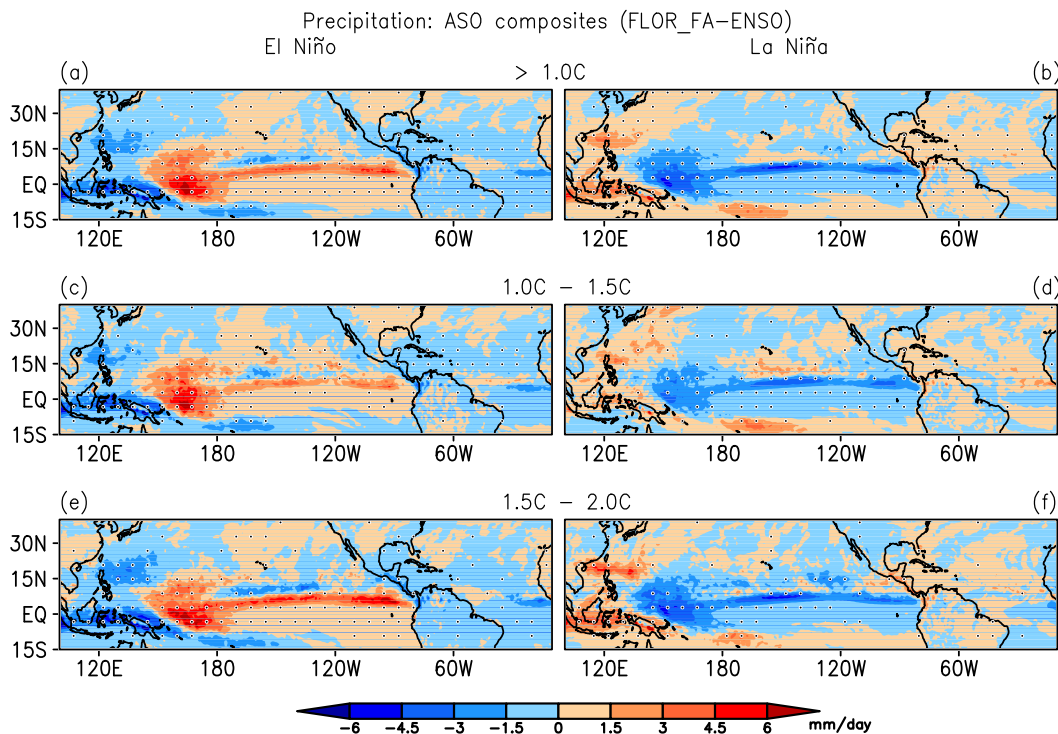| Criteria	El Niño	Rate of El Niño	La Niña	Rate of La Niña
>1.0°C	17	0.17 ± 0.07	19	0.19 ± 0.07
1.0°–1.5°C	8	0.08 ± 0.05	8	0.08 ± 0.05
1.5°–2.0°C	8	0.08 ± 0.05	5	0.05 ± 0.04

FIG. 11. As in Fig. 5, but for FLOR-FA_enso. The number of years over which composites are based is noted in Table 4. The dotted regions indicate the 5% significance level.

the TC density in the southeast of the WNP does show improvement with improved representation of the magnitude of the SSTs in the tropical Pacific Ocean. This experiment suggests that an improved ENSO variability yields a better ENSO–TC relation, similar to observations. The composites of precipitation and of the number of days with VWS $> 10\,\mathrm{m\,s}^{-1}$ also support the mechanistic hypothesis proposed in the previous section for the differences in the ENSO-related TC activity between FLOR and FLOR-FA. The maximum of convection in FLOR-FA_enso is located west of the date line, which is consistent with the location of ENSO-related TC activity in the southeast of the WNP (Figs. 10a and 11a). The composite of number of days with VWS $> 10\,\mathrm{m\,s}^{-1}$ during El Niño also does not show high number of days at the mean genesis location in the ENP (Fig. 12a), which contributes to a more realistic representation of the suppression of TC activity during El Niño. In the case of the La Niña composite, the number of days is not as reduced as in FLOR to favor TC activity (Figs. 10b and 12b). The results from this experiment demonstrate that the differences between FLOR and FLOR-FA in the southeastern part of the WNP and ENP relative to observations arise from the stronger ENSO in FLOR.

4. Conclusions and discussion

In this study, we have investigated the sensitivity of the regional TC activity in the Pacific and Atlantic Oceans to strong ENSO events using long simulations from coupled climate models. First, we assessed the ability of the coupled climate model, GFDL FLOR to simulate the relationship between the ENSO and regional TC activity in the Pacific and Atlantic Oceans. FLOR showed biases in the simulation of the ENSO–TC relationship compared to observations. During El Niño, TC activity in the WNP is shifted eastward and is stronger than observed in the eastern part of the basin. It also failed to simulate TC activity in the west Atlantic. During La Niña, FLOR simulates enhanced TC activity in the ENP in contrast to observations, which show reduced TC activity. However, the flux-adjusted version of FLOR, FLOR-FA shows realistic simulation of the observed relationship between ENSO and TC activity.

Thus, we use FLOR-FA for our investigation to understand the sensitivity of regional TCs to strong ENSO events and the associated mechanisms are summarized in Fig. 13 for El Niño events only. We suggest that TCs exhibit a nonlinear response to the strength of ENSO in the tropical eastern North Pacific (ENP) but a quasi-linear response in the tropical west North Pacific (WNP)
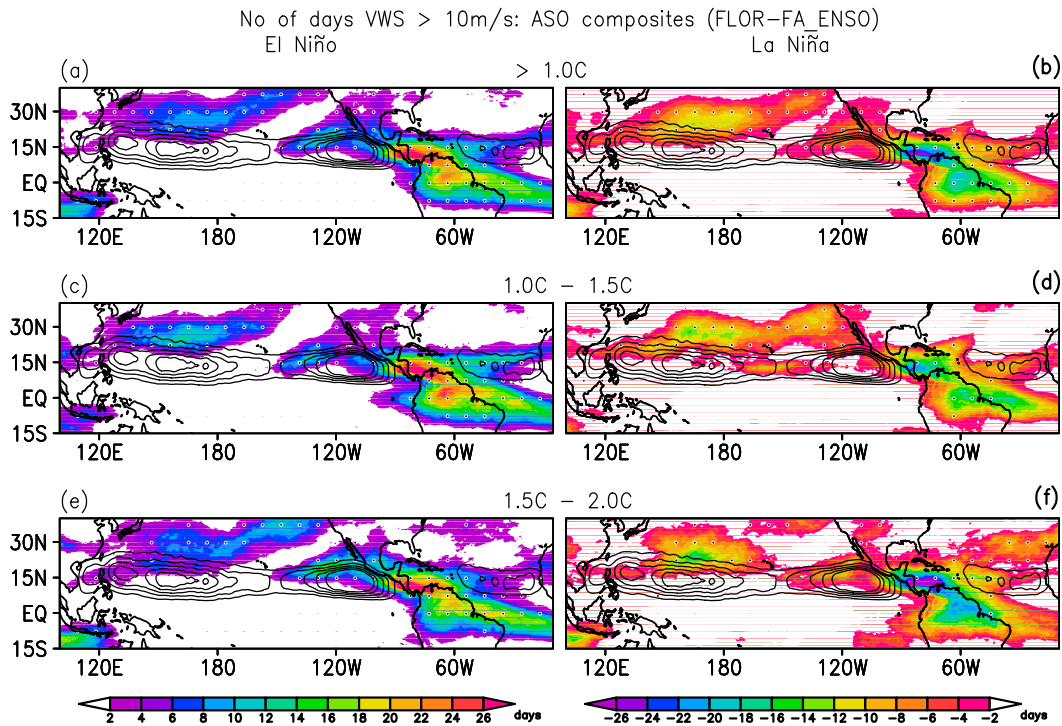
FIG. 12. As in Fig. 7, but for FLOR-FA_enso. The number of years over which composites are based is noted in Table 4. The dotted regions indicate the 5% significance level.

and tropical North Atlantic. However, FLOR fails to capture the nonlinear response in the ENP (cf. Figs. 14 and 15). We showed that the location and magnitude of regional TC activity in the tropical North Pacific and

Atlantic Oceans are sensitive to the strength of El Niño. A stronger El Niño shows an eastward shift of TC activity in the southeastern part of WNP. This shift in TC activity was shown to be related to a shift in the location
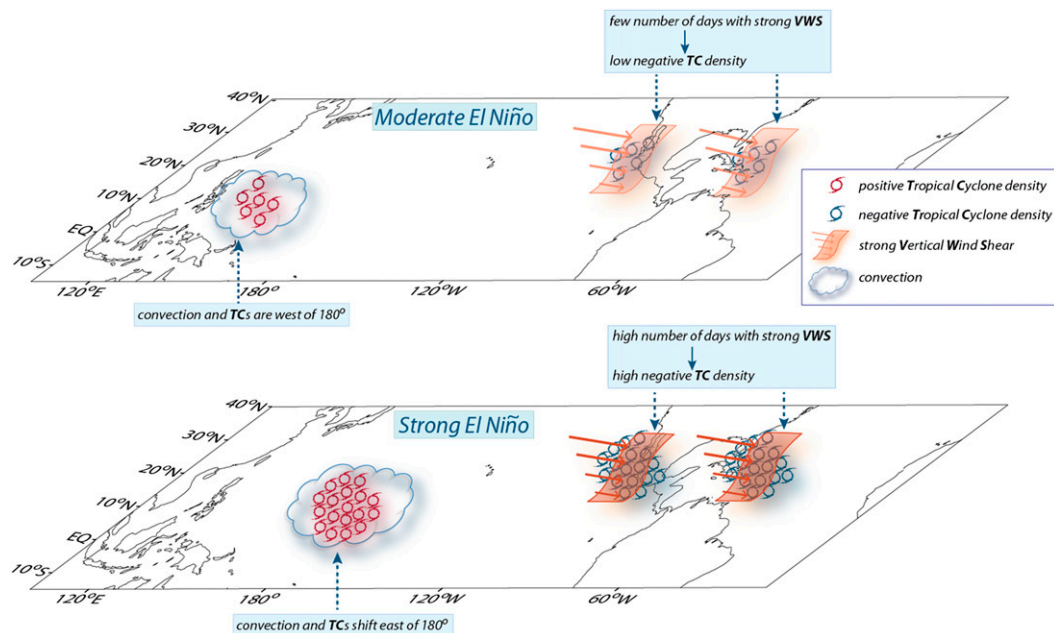

FIG. 13. Schematic showing the effect of moderate and strong El Niño on TC activity.
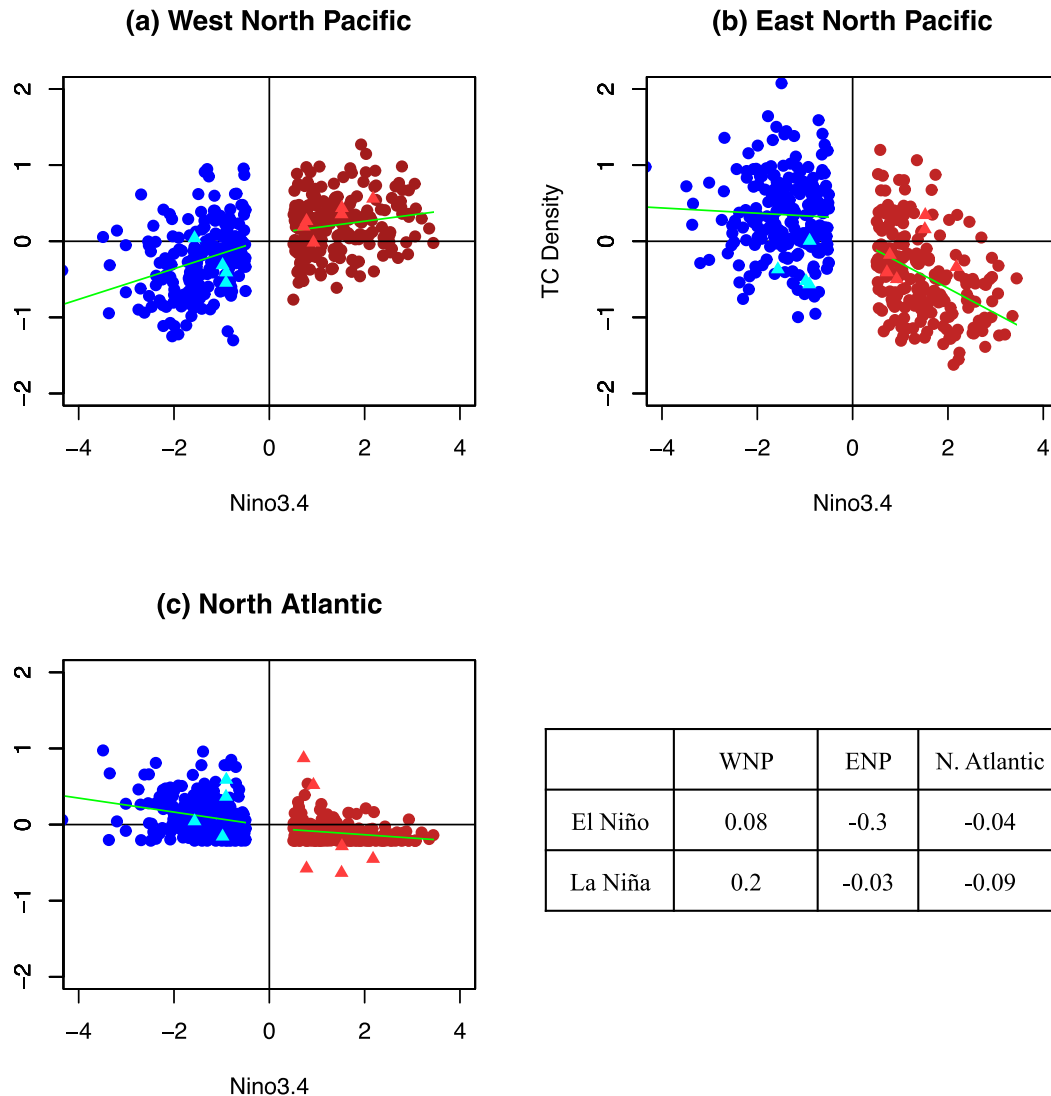
(a) West North Pacific

(b) East North Pacific

(c) North Atlantic

	WNP	ENP	N. Atlantic
El Niño	0.08	-0.3	-0.04
La Niña	0.2	-0.03	-0.09

FIG. 14. Scatterplot of Niño-3.4 and area-averaged TC density index (FLOR) over (a) the west North Pacific (10°–30°N, 130°E–150°W), (b) the east North Pacific (10°–30°N, 130°–100°W), and (c) the North Atlantic (10°–30°N, 95°–60°W). Red (blue) dots represent events with Niño-3.4 > 0.5°C (< −0.5°C) corresponding to El Niño (La Niña) in FLOR. Light red (blue) triangles represent events with Niño-3.4 > 0.5°C (< −0.5°C) corresponding to El Niño (La Niña) in observations. The linear regression coefficients are shown in the table for FLOR.

of atmospheric convection. Strong El Niño events have a tendency to shift the convection to the east (Fig. 13). This further leads to an eastward shift in the environmental conditions favorable for TC activity such as weak VWS and thus causing an eastward shift in TC activity. Strong El Niño events also tend to enhance the inhibition of TCs in the ENP and in the North Atlantic by increasing the number of days with strong VWS (Fig. 13). However, we showed that TC activity in the North Pacific is insensitive to the increase in the strength of La Niña events. Tropical cyclone activity does not show a distinct shift in the longitudinal location in the

WNP with an increase in the strength of La Niña as compared to El Niño. The magnitude of TC activity in the ENP is also insensitive to the strength of La Niña. The sensitivity of TCs to strong La Niña events could only be seen in the North Atlantic, where stronger La Niña events tend to reduce the number of days with strong VWS, favoring TC activity.

We also investigated the reasons for the biases in the simulation of the ENSO–TC relationship in FLOR. We hypothesized that the biases in the ENSO–TC relationship in the North Pacific arise from an excessively strong ENSO in FLOR. An overly strong El Niño event

(a) West North Pacific

(b) East North Pacific

(c) North Atlantic

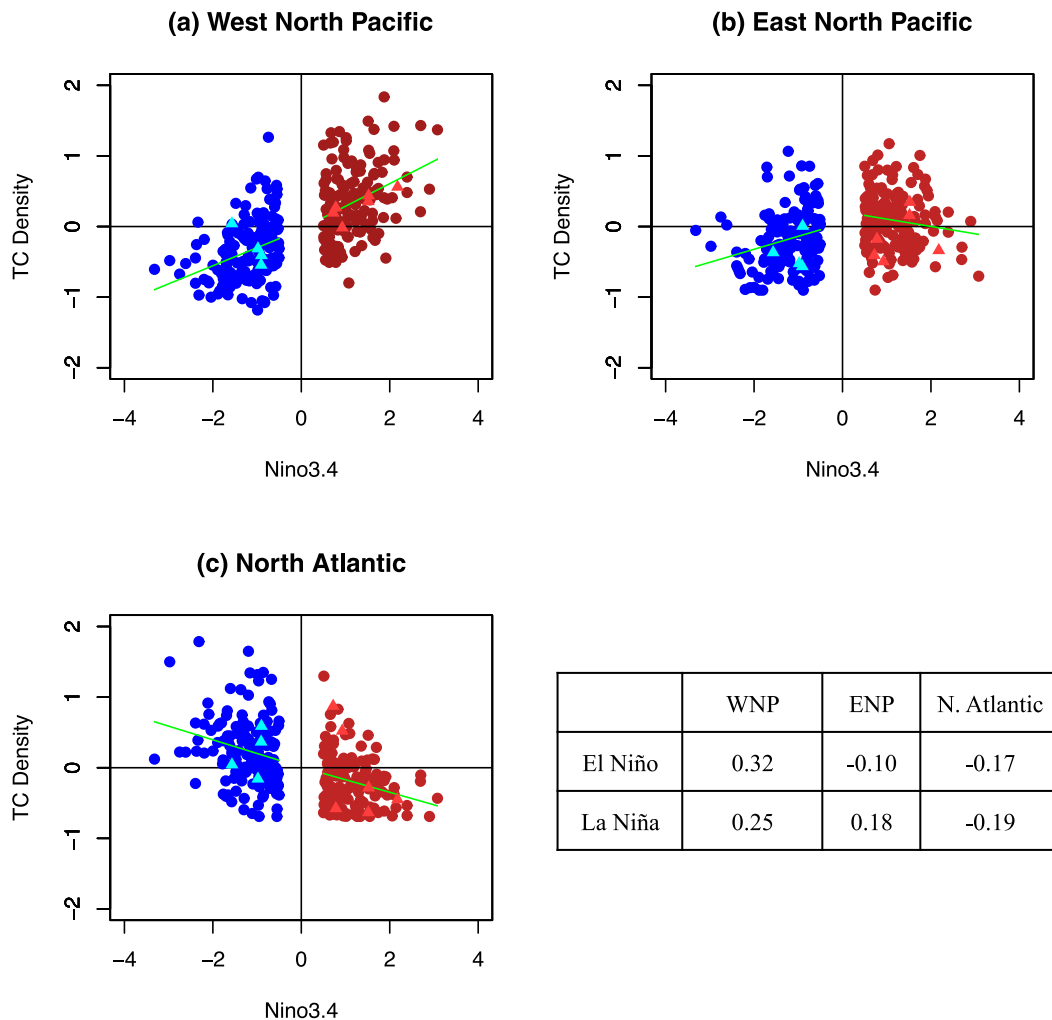|	WNP	ENP	N. Atlantic
El Niño	0.32	-0.10	-0.17
La Niña	0.25	0.18	-0.19

FIG. 15. As in Fig. 14, but for FLOR-FA.

causes an excessive eastward shift in convection in FLOR compared to observations and FLOR-FA, leading to an erroneous shift in the location of TCs. In ENP, a strong El Niño increases the number of days with strong VWS in FLOR, leading to stronger than observed inhibition of TC activity in the ENP (Fig. 14b). Strong La Niña events in FLOR decrease the number of days with strong VWS and, hence, favor TC activity in contrast to observations and FLOR-FA. Using perturbation experiment (FLOR_FA-enso) with a realistic representation of the amplitude of ENSO, partly corrects for the biases in FLOR, supporting our hypothesis.

Further, we showed that FLOR also fails to simulate the signature of ENSO–TC teleconnection in the west Atlantic during both the El Niño and La Niña events. We suggested that these biases in the west Atlantic teleconnection might be attributed to the biases in the FLOR simulation of the mean genesis density and track

density in the west Atlantic. The mean genesis and thus track density in FLOR is shifted to the east of the west Atlantic relative to observations, thus causing the response of TCs to ENSO to also shift eastward. FLOR-FA shows improvement in the simulation of genesis and track location and thus it has a better simulation of the location of teleconnection with enhanced TC activity in the west Atlantic during La Niña and a reduced activity during El Niño.

There are twofold benefits from the evaluation of the ability of the state-of-the-art coupled climate model to simulate the ENSO–TC relationship. This study helps us to recognize the biases in the simulations and work toward its improvements. Although this study is based on a single model, FLOR, these results could be useful to other climate models that may have comparable biases in the simulation of the amplitude of ENSO and the genesis location of TCs. This study provides insights

on how the biases in the simulation of ENSO and genesis location of TCs can reflect on the biases in the simulation of ENSO–TC teleconnections. Our results also suggest that coupled climate models with improved simulation of ENSO and its relationship to regional TC activity would aid in better prediction of TCs as shown in Vecchi et al. (2014). Finally, using long control simulations, we showed that the regional TC activity is sensitive to the strength of the ENSO event. Given that the frequency of extreme ENSO precipitation events is projected to increase in warming scenarios (Power et al. 2013; Wittenberg 2015; Cai et al. 2014, 2015), this work can help us to understand the effects of extreme ENSO events on the regional TC activity, which further helps us to understand the connections between a changing climate and tropical cyclones.

REFERENCES

Bove, M. C., J. B. Elsner, C. W. Landsea, X. Niu, and J. J. O'Brien, 1998: Effect of El Niño on U.S. landfalling hurricanes, revisited. *Bull. Amer. Meteor. Soc.*, **79**, 2477–2482, doi:10.1175/1520-0477(1998)079<2477:EOENOO>2.0.CO;2.

Cai, W., and Coauthors, 2014: Increasing frequency of extreme El Niño events due to greenhouse warming. *Nat. Climate Change*, **4**, 111–116, doi:10.1038/nclimate2100.

——, and Coauthors, 2015: Increased frequency of extreme La Niña events under greenhouse warming. *Nat. Climate Change*, **5**, 132–137, doi:10.1038/nclimate2492.

Camargo, S. J., K. A. Emanuel, and A. H. Sobel, 2007: Use of a genesis potential index to diagnose ENSO effects on tropical cyclone genesis. *J. Climate*, **20**, 4819–4834, doi:10.1175/JCLI4282.1.

Chan, J. C. L., 1985: Tropical cyclone activity in the northwest Pacific in relation to the El Niño/Southern Oscillation phenomenon. *Mon. Wea. Rev.*, **113**, 599–606, doi:10.1175/1520-0493(1985)113<0599:TCAITN>2.0.CO;2.

Chen, G., 2011: How does shifting Pacific Ocean warming modulate on tropical cyclone frequency over the South China Sea? *J. Climate*, **24**, 4695–4700, doi:10.1175/2011JCLI4140.1.

——, and C. Y. Tam, 2010: Different impacts of two kinds of Pacific Ocean warming on tropical cyclone frequency over the western North Pacific. *Geophys. Res. Lett.*, **37**, L01803, doi:10.1029/2009GL041708.

Chia, H. H., and C. F. Ropelewski, 2002: The interannual variability in the genesis location of tropical cyclones in the northwest Pacific. *J. Climate*, **15**, 2934–2944, doi:10.1175/1520-0442(2002)015<2934:TIVITG>2.0.CO;2.

Chu, P.-S., 2004: ENSO and tropical cyclone activity. *Hurricanes and Typhoons, Past, Present and Future*, R. J. Murnane and K.-B. Liu, Eds., Columbia University Press, 297–332.

——, and J. Wang, 1997: Tropical cyclone occurrences in the vicinity of Hawaii: Are the differences between El Niño and non–El Niño years significant? *J. Climate*, **10**, 2683–2689, doi:10.1175/1520-0442(1997)010<2683:TCOITV>2.0.CO;2.

Clark, J. D., and P.-S. Chu, 2002: Interannual variation of tropical cyclone activity over the central North Pacific. *J. Meteor. Soc. Japan*, **80**, 403–418, doi:10.2151/jmsj.80.403.

Delworth, T. L., F. Zeng, A. Rosati, G. A. Vecchi, and A. T. Wittenberg, 2015: A link between the hiatus in global warming and North American drought. *J. Climate*, **28**, 3834–3845, doi:10.1175/JCLI-D-14-00616.1.

Dong, K., 1988: El Niño and tropical cyclone frequency in the Australian region and the northwest Pacific. *Aust. Meteor. Mag.*, **28**, 219–225.

Goldenberg, S. B., and L. J. Shapiro, 1996: Physical mechanisms for the association of El Niño and West African rainfall with Atlantic major hurricane activity. *J. Climate*, **9**, 1169–1187, doi:10.1175/1520-0442(1996)009<1169:PMFTAO>2.0.CO;2.

Gray, W. M., 1984: Atlantic seasonal hurricane frequency. Part I: El Niño and 30-mb quasi-biennial oscillation influences. *Mon. Wea. Rev.*, **112**, 1649–1668, doi:10.1175/1520-0493(1984)112<1649:ASHFPI>2.0.CO;2.

Irwin, R. P., and R. Davis, 1999: The relationship between the Southern Oscillation Index and tropical cyclone tracks in the eastern North Pacific. *Geophys. Res. Lett.*, **26**, 2251–2254, doi:10.1029/1999GL900533.

Jia, L., and Coauthors, 2015: Improved seasonal prediction of temperature and precipitation over land in a high-resolution GFDL climate model. *J. Climate*, **28**, 2044–2062, doi:10.1175/JCLI-D-14-00112.1.

Kim, H.-M., P. J. Webster, and J. A. Curry, 2009: Impact of shifting patterns of Pacific Ocean warming on North Atlantic tropical cyclones. *Science*, **325**, 77–80, doi:10.1126/science.1174062.

——, ——, and ——, 2011: Modulation of North Pacific tropical cyclone activity by three phases of ENSO. *J. Climate*, **24**, 1839–1849, doi:10.1175/2010JCLI3939.1.

Kim, H.-S., G. A. Vecchi, T. R. Knutson, W. G. Anderson, T. L. Delworth, A. Rosati, F. Zeng, and M. Zhao, 2014: Tropical cyclone simulation and response to CO_2 doubling in the GFDL CM2.5 high-resolution coupled climate model. *J. Climate*, **27**, 8034–8054, doi:10.1175/JCLI-D-13-00475.1.

Knapp, K. R., M. C. Kruk, D. H. Levinson, H. J. Diamond, and C. J. Neuman, 2010: The International Best Track Archive for Climate Stewardship (IBTrACS). *Bull. Amer. Meteor. Soc.*, **91**, 363–376, doi:10.1175/2009BAMS2755.1.

Krishnamurthy, L., G. A. Vecchi, R. Msadek, A. Wittenberg, T. L. Delworth, and F. Zeng, 2015: The seasonality of the Great Plains low-level jet and ENSO relationship. *J. Climate*, **28**, 4525–4544, doi:10.1175/JCLI-D-14-00590.1.

Landsea, C. W., 2000: El Niño–Southern Oscillation and the seasonal predictability of tropical cyclones. *El Niño: Impacts of Multiscale Variability on Natural Ecosystems and Society*, H. F. Diaz and V. Markgraf, Eds., Cambridge University Press, 149–181.

Lengaigne, M., and G. A. Vecchi, 2010: Contrasting the termination of moderate and extreme El Nino events in coupled general circulation models. *Climate Dyn.*, **35**, 299–313, doi:10.1007/s00382-009-0562-3.

Li, C., and C. Wang, 2014: Simulated impacts of two types of ENSO events on tropical cyclone activity in the western

North Pacific: Large-scale atmospheric response. *Climate Dyn.*, **42**, 2727–2743, doi:10.1007/s00382-013-1999-y.

Murakami, H., and Coauthors, 2012: Future changes in tropical cyclone activity projected by the new high-resolution MRI-AGCM. *J. Climate*, **25**, 3237–3260, doi:10.1175/JCLI-D-11-00415.1.

——, and Coauthors, 2015: Simulation and prediction of category 4 and 5 hurricanes in the high-resolution GFDL HiFLOR coupled climate model. *J. Climate*, **28**, 9058–9079, doi:10.1175/JCLI-D-15-0216.1.

Peduzzi, P., B. Chatenoux, H. Dao, A. De Bono, C. Herold, J. Kossin, F. Mouton, and O. Nordbeck, 2012: Global trends in tropical cyclone risk. *Nat. Climate Change*, **2**, 289–294, doi:10.1038/nclimate1410.

Pielke, R. A., Jr., and C. W. Landsea, 1999: La Niña, El Niño, and Atlantic hurricane damages in the United States. *Bull. Amer. Meteor. Soc.*, **80**, 2027–2033, doi:10.1175/1520-0477(1999)080<2027:LNAENO>2.0.CO;2.

——, J. Gratz, C. Landsea, D. Collins, M. Saunders, and R. Musulin, 2008: Normalized hurricane damage in the United States: 1900–2005. *Nat. Hazards Rev.*, **9**, 29–42, doi:10.1061/(ASCE)1527-6988(2008)9:1(29).

Power, S., F. Delage, C. Chung, G. Kociuba, and K. Keay, 2013: Robust twenty-first-century projections of El Niño and related precipitation variability. *Nature*, **502**, 541–545, doi:10.1038/nature12580.

Rayner, N. A., D. E. Parker, E. B. Horton, C. K. Folland, L. V. Alexander, D. P. Rowell, E. C. Kent, and A. Kaplan, 2003: Global analyses of sea surface temperature, sea ice, and night marine air temperature since the late nineteenth century. *J. Geophys. Res.*, **108**, 4407, doi:10.1029/2002JD002670.

Rienecker, M. M., and Coauthors, 2011: MERRA: NASA's Modern-Era Retrospective Analysis for Research and Applications. *J. Climate*, **24**, 3624–3648, doi:10.1175/JCLI-D-11-00015.1.

Schroeder, T. A., and Z.-P. Yu, 1995: Interannual variability of central Pacific tropical cyclones. Preprints, *21st Conf. on Hurricanes and Tropical Meteorology*, Miami, FL, Amer. Meteor. Soc., 437–439.

Shapiro, L. J., 1987: Month-to-month variability of the Atlantic tropical circulation and its relationship to tropical storm formation. *Mon. Wea. Rev.*, **115**, 2598–2614, doi:10.1175/1520-0493(1987)115<2598:MTMVOT>2.0.CO;2.

Tang, B. H., and J. D. Neelin, 2004: ENSO influence on Atlantic hurricanes via tropospheric warming. *Geophys. Res. Lett.*, **31**, L24204, doi:10.1029/2004GL021072.

Vecchi, G. A., 2006: The termination of the 1997–98 El Niño. Part II: Mechanisms of atmospheric change. *J. Climate*, **19**, 2647–2664, doi:10.1175/JCLI3780.1.

——, and D. E. Harrison, 2006: The termination of the 1997–98 El Niño. Part I: Mechanisms of oceanic change. *J. Climate*, **19**, 2633–2646, doi:10.1175/JCLI3776.1.

——, and Coauthors, 2014: On the seasonal forecasting of regional tropical cyclone activity. *J. Climate*, **27**, 7994–8016, doi:10.1175/JCLI-D-14-00158.1.

Villarini, G., R. Goska, J. A. Smith, and G. A. Vecchi, 2014: North Atlantic tropical cyclones and U.S. flooding. *Bull. Amer. Meteor. Soc.*, **95**, 1381–1388, doi:10.1175/BAMS-D-13-00060.1.

Vimont, D. J., and J. P. Kossin, 2007: The Atlantic meridional mode and hurricane activity. *Geophys. Res. Lett.*, **34**, L07709, doi:10.1029/2007GL029683.

Walsh, K., M. Fiorino, C. Landsea, and K. McInnes, 2007: Objectively determined resolution-dependent threshold criteria for the detection of tropical cyclones in climate models and reanalyses. *J. Climate*, **20**, 2307–2314, doi:10.1175/JCLI4074.1.

Wang, B., and J. C. L. Chan, 2002: How strong ENSO events affect tropical storm activity over the western North Pacific. *J. Climate*, **15**, 1643–1658, doi:10.1175/1520-0442(2002)015<1643:HSEEAT>2.0.CO;2.

Wang, C., C. Li, M. Mu, and W. Duan, 2013: Seasonal modulations of different impacts of two types of ENSO events on tropical cyclone activity in the western North Pacific. *Climate Dyn.*, **40**, 2887–2902, doi:10.1007/s00382-012-1434-9.

Wang, H., and Coauthors, 2014: How well do global climate models simulate the variability of Atlantic tropical cyclones associated with ENSO? *J. Climate*, **27**, 5673–5692, doi:10.1175/JCLI-D-13-00625.1.

Wang, X., W. Zhou, C. Li, and D. Wang, 2014: Comparison of the impact of two types of El Niño on tropical cyclone genesis over the South China Sea. *Int. J. Climatol.*, **34**, 2651–2660, doi:10.1002/joc.3865.

Wittenberg, A. T., 2009: Are historical records sufficient to constrain ENSO simulations? *Geophys. Res. Lett.*, **36**, L12702, doi:10.1029/2009GL038710.

——, 2015: Low-frequency variations of ENSO. *U.S. CLIVAR Variations*, **13** (1), 26–31. [Available online at http://www.gfdl.noaa.gov/~atw/yr/2015/wittenberg_variations2015.pdf.]

Wu, G., and N.-C. Lau, 1992: A GCM simulation of the relationship between tropical-storm formation and ENSO. *Mon. Wea. Rev.*, **120**, 958–977, doi:10.1175/1520-0493(1992)120<0958:AGSOTR>2.0.CO;2.

Xie, P., and P. A. Arkin, 1997: Global precipitation: A 17-year monthly analysis based on gauge observations, satellite estimates, and numerical model outputs. *Bull. Amer. Meteor. Soc.*, **78**, 2539–2558, doi:10.1175/1520-0477(1997)078<2539:GPAYMA>2.0.CO;2.

Zhang, W., H. Graf, Y. Leung, and M. Herzog, 2012: Different El Niño types and tropical cyclone landfall in East Asia. *J. Climate*, **25**, 6510–6523, doi:10.1175/JCLI-D-11-00488.1.

Zhao, M., I. M. Held, S.-J. Lin, and G. A. Vecchi, 2009: Simulations of global hurricane climatology, interannual variability, and response to global warming using a 50-km resolution GCM. *J. Climate*, **22**, 6653–6678, doi:10.1175/2009JCLI3049.1.